



ELSEVIER

14 September 2000

PHYSICS LETTERS B

Physics Letters B 489 (2000) 38–54

www.elsevier.nl/locate/npe

Limits on the masses of supersymmetric particles at $\sqrt{s} = 189$ GeV

DELPHI Collaboration

P. Abreu^u, W. Adam^{ay}, T. Adye^{ak}, P. Adzic^k, I. Ajinenko^{aq}, Z. Albrecht^q,
T. Alderweireld^b, G.D. Alekseev^p, R. Alemany^{ax}, T. Allmendinger^q, P.P. Allport^v,
S. Almehed^x, U. Amaldi^{ab}, N. Amapane^{at}, S. Amato^{av}, E.G. Anassontzis^c,
P. Andersson^{as}, A. Andreazza^{aa}, S. Andringa^u, P. Antilogus^y, W-D. Apel^q,
Y. Arnoudⁿ, B. Åsman^{as}, J-E. Augustin^w, A. Augustinusⁱ, P. Baillonⁱ,
A. Ballestrero^{at}, P. Bambade^{i,s}, F. Barao^u, G. Barbiellini^{au}, R. Barbier^y,
D.Y. Bardin^p, G. Barker^q, A. Baroncelli^{am}, M. Battaglia^o, M. Baubillier^w,
K-H. Becks^{ba}, M. Begalli^f, A. Behrmann^{ba}, P. Beilliere^h, Yu. Belokopytovⁱ,
N.C. Benekos^{af}, A.C. Benvenuti^e, C. Beratⁿ, M. Berggren^w, L. Berntzon^{as},
D. Bertrand^b, M. Besancon^{an}, M.S. Bilenky^p, M-A. Bizouard^s, D. Bloch^j,
H.M. Blom^{ae}, M. Bonesini^{ab}, M. Boonekamp^{an}, P.S.L. Booth^v, G. Borisov^s,
C. Bosio^{ap}, O. Botner^{aw}, E. Boudinov^{ae}, B. Bouquet^s, C. Bourdarios^s,
T.J.V. Bowcock^v, I. Boyko^p, I. Bozovic^k, M. Bozzo^m, M. Bracko^{ar}, P. Branchini^{am},
R.A. Brenner^{aw}, P. Bruckmanⁱ, J-M. Brunet^h, L. Bugge^{ag}, T. Buran^{ag},
B. Buschbeck^{ay}, P. Buschmann^{ba}, S. Cabrera^{ax}, M. Caccia^{aa}, M. Calvi^{ab},
T. Camporesiⁱ, V. Canale^{al}, F. Carenaⁱ, L. Carroll^v, C. Caso^m,
M.V. Castillo Gimenez^{ax}, A. Cattaiⁱ, F.R. Cavallo^e, Ph. Charpentierⁱ,
P. Checchia^{aj}, G.A. Chelkov^p, R. Chierici^{at}, P. Chliapnikov^{i,aq}, P. Chochula^g,
V. Chorowicz^y, J. Chudoba^{ad}, K. Cieslik^r, P. Collinsⁱ, R. Contri^m,
E. Cortina^{ax}, G. Cosme^s, F. Cossuttiⁱ, M. Costa^{ax}, H.B. Crawley^a,
D. Crennell^{ak}, G. Crosetti^m, J. Cuevas Maestro^{ah}, S. Czellar^o,
J. D'Hondt^b, J. Dalmau^{as}, M. Davenportⁱ, W. Da Silva^w, G. Della Ricca^{au},
P. Delpierre^z, N. Demaria^{at}, A. De Angelis^{au}, W. De Boer^q, C. De Clercq^b,
B. De Lotto^{au}, A. De Minⁱ, L. De Paula^{av}, H. Dijkstraⁱ, L. Di Ciaccio^{al},
J. Dolbeau^h, K. Doroba^{az}, M. Dracos^j, J. Drees^{ba}, M. Dris^{af}, G. Eigen^d,
T. Ekelof^{aw}, M. Ellert^{aw}, M. Elsingⁱ, J-P. Engel^j, M. Espirito Santoⁱ,

G. Fanourakis^k, D. Fassouliotis^k, M. Feindt^q, J. Fernandez^{ao}, A. Ferrer^{ax},
 E. Ferrer-Ribas^s, F. Ferro^m, A. Firestone^a, U. Flagmeyer^{ba}, H. Foethⁱ, E. Fokitis^{af},
 F. Fontanelli^m, B. Franek^{ak}, A.G. Frodesen^d, R. Fruhwirth^{ay}, F. Fulda-Quenzer^s,
 J. Fuster^{ax}, A. Galloni^v, D. Gamba^{at}, S. Gamblin^s, M. Gandelman^{av}, C. Garcia^{ax},
 C. Gasparⁱ, M. Gaspar^{av}, U. Gasparini^{aj}, Ph. Gavilletⁱ, E.N. Gazis^{af}, D. Gele^j,
 T. Gerasis^k, L. Gerdyukov^{aq}, N. Ghodbane^y, I. Gil^{ax}, F. Glege^{ba}, R. Gokieli^{i,az},
 B. Golob^{i,ar}, G. Gomez-Ceballos^{ao}, P. Goncalves^u, I. Gonzalez Caballero^{ao},
 G. Gopal^{ak}, L. Gorn^a, Yu. Gouz^{aq}, V. Gracco^m, J. Grahl^a, E. Graziani^{am},
 P. Gris^{an}, G. Grosdidier^s, K. Grzelak^{az}, J. Guy^{ak}, C. Haag^q, F. Hahnⁱ,
 S. Hahn^{ba}, S. Haiderⁱ, A. Hallgren^{aw}, K. Hamacher^{ba}, J. Hansen^{ag}, F.J. Harris^{ai},
 F. Hauler^q, V. Hedberg^{i,x}, S. Heising^q, J.J. Hernandez^{ax}, P. Herquet^b, H. Herrⁱ,
 E. Higon^{ax}, S-O. Holmgren^{as}, P.J. Holt^{ai}, S. Hoorelbeke^b, M. Houlden^v,
 J. Hrubec^{ay}, M. Huber^q, G.J. Hughes^v, K. Hultqvist^{i,as}, J.N. Jackson^v,
 R. Jacobssonⁱ, P. Jalocha^r, R. Janik^g, Ch. Jarlskog^x, G. Jarlskog^x, P. Jarry^{an},
 B. Jean-Marie^s, D. Jeans^{ai}, E.K. Johansson^{as}, P. Jonsson^y, C. Joramⁱ, P. Juillot^j,
 L. Jungermann^q, F. Kapusta^w, K. Karafasoulis^k, S. Katsanevas^y, E.C. Katsoufis^{af},
 R. Keranen^q, G. Kernel^{ar}, B.P. Kersevan^{ar}, Yu. Khokhlov^{aq}, B.A. Khomenko^p,
 N.N. Khovanski^p, A. Kiiskinen^o, B. King^v, A. Kinvig^v, N.J. Kjaerⁱ, O. Klapp^{ba},
 P. Kluit^{ae}, P. Kokkinias^k, V. Kostioukhine^{aq}, C. Kourkoumelis^c, O. Kouznetsov^p,
 M. Krammer^{ay}, E. Kriznic^{ar}, Z. Krumstein^p, P. Kubinec^g, J. Kurowska^{az},
 K. Kurvinen^o, J.W. Lamsa^a, D.W. Lane^a, J-P. Laugier^{an}, R. Lauhakangas^o,
 G. Leder^{ay}, F. Ledroitⁿ, L. Leinonen^{as}, A. Leisos^k, R. Leitner^{ad}, G. Lenzen^{ba},
 V. Lepeltier^s, T. Lesiak^r, M. Lethuillier^y, J. Libby^{ai}, W. Liebig^{ba}, D. Likoⁱ,
 A. Lipniacka^{as}, I. Lippi^{aj}, B. Loerstad^x, J.G. Loken^{ai}, J.H. Lopes^{av}, J.M. Lopez^{ao},
 R. Lopez-Fernandezⁿ, D. Loukas^k, P. Lutz^{an}, L. Lyons^{ai}, J. MacNaughton^{ay},
 J.R. Mahon^f, A. Maio^u, A. Malek^{ba}, S. Maltezos^{af}, V. Malychev^p, F. Mandl^{ay},
 J. Marco^{ao}, R. Marco^{ao}, B. Marechal^{av}, M. Margoni^{aj}, J-C. Marinⁱ, C. Mariottiⁱ,
 A. Markou^k, C. Martinez-Riveroⁱ, S. Marti i Garciaⁱ, J. Masik^l,
 N. Mastroiannopoulos^k, F. Matorras^{ao}, C. Matteuzzi^{ab}, G. Matthiae^{al},
 F. Mazzucato^{aj}, M. Mazzucato^{aj}, M. Mc Cubbin^v, R. Mc Kay^a, R. Mc Nulty^v,
 G. Mc Pherson^v, E. Merleⁿ, C. Meroni^{aa}, W.T. Meyer^a, E. Miglioreⁱ,
 L. Mirabito^y, W.A. Mitaroff^{ay}, U. Mjoernmark^x, T. Moa^{as}, M. Moch^q,
 R. Moeller^{ac}, K. Moenig^{i,l}, M.R. Monge^m, D. Moraes^{av}, P. Morettini^m,
 G. Morton^{ai}, U. Mueller^{ba}, K. Muenich^{ba}, M. Mulders^{ae}, C. Mulet-Marquisⁿ,
 L.M. Mundim^f, R. Muresan^x, W.J. Murray^{ak}, B. Muryn^r, G. Myatt^{ai},
 T. Myklebust^{ag}, F. Naraghiⁿ, M. Nassiakou^k, F.L. Navarra^e, K. Nawrocki^{az},
 P. Negri^{ab}, N. Neufeld^{ay}, R. Nicolaidou^{an}, B.S. Nielsen^{ac}, P. Niezurawski^{az},
 M. Nikolenko^{j,p}, V. Nomokonov^o, A. Nygren^x, V. Obraztsov^{aq}, A.G. Olshevski^p,

A. Onofre^u, R. Orava^o, G. Orazi^j, K. Osterbergⁱ, A. Ouraou^{an}, A. Oyanguren^{ax},
M. Paganoni^{ab}, S. Paiano^e, R. Pain^w, R. Paiva^u, J. Palacios^{ai}, H. Palka^r,
Th.D. Papadopoulou^{af}, L. Papeⁱ, C. Parkesⁱ, F. Parodi^m, U. Parzefall^v,
A. Passeri^{am}, O. Passon^{ba}, T. Pavel^x, M. Pegoraro^{aj}, L. Peralta^u, M. Pernicka^{ay},
A. Perrotta^e, C. Petridou^{au}, A. Petrolini^m, H.T. Phillips^{ak}, F. Pierre^{an}, M. Pimenta^u,
E. Piotto^{aa}, T. Podobnik^{ar}, V. Poireau^{an}, M.E. Pol^f, G. Polok^r, P. Poropat^{au},
V. Pozdniakov^p, P. Privitera^{al}, N. Pukhaeva^p, A. Pullia^{ab}, D. Radojicic^{ai},
S. Ragazzi^{ab}, H. Rahmani^{af}, J. Rames^l, P.N. Ratoff^t, A.L. Read^{ag}, P. Rebecchiⁱ,
N.G. Redaelli^{ab}, M. Regler^{ay}, J. Rehn^q, D. Reid^{ae}, P. Reinertsen^d, R. Reinhardt^{ba},
P.B. Renton^{ai}, L.K. Resvanis^c, F. Richard^s, J. Ridky^l, G. Rinaudo^{at},
I. Ripp-Baudot^j, A. Romero^{at}, P. Ronchese^{aj}, E.I. Rosenberg^a, P. Rosinsky^g,
P. Roudeau^s, T. Rovelli^e, V. Ruhlmann-Kleider^{an}, A. Ruiz^{ao}, H. Saarikko^o,
Y. Sacquin^{an}, A. Sadovsky^p, G. Sajotⁿ, J. Salt^{ax}, D. Sampsonidis^k,
M. Sannino^m, A. Savoy-Navarro^w, Ph. Schwemling^w, B. Schwering^{ba},
U. Schwickerath^q, F. Scuri^{au}, P. Seager^t, Y. Sedykh^p, A.M. Segar^{ai},
N. Seibert^q, R. Sekulin^{ak}, G. Sette^m, R.C. Shellard^f, M. Siebel^{ba}, L. Simard^{an},
F. Simonetto^{aj}, A.N. Sisakian^p, G. Smadja^y, N. Smirnov^{aq}, O. Smirnova^x,
G.R. Smith^{ak}, A. Sokolov^{aq}, A. Sopczak^q, R. Sosnowski^{az}, T. Spassovⁱ, E. Spiriti^{am},
S. Squarcia^m, C. Stanescu^{am}, M. Stanitzki^q, K. Stevenson^{ai}, A. Stocchi^s, J. Strauss^{ay},
R. Strub^j, B. Stugu^d, M. Szczekowski^{az}, M. Szeptycka^{az}, T. Tabarelli^{ab},
A. Taffard^v, O. Tchikilev^{aq}, F. Tegenfeldt^{aw}, F. Terranova^{ab}, J. Timmermans^{ae},
N. Tinti^e, L.G. Tkatchev^p, M. Tobin^v, S. Todorovaⁱ, B. Tome^u, A. Tonazzoⁱ,
L. Tortora^{am}, P. Tortosa^{ax}, G. Transtomer^x, D. Treilleⁱ, G. Tristram^h,
M. Trochimczuk^{az}, C. Troncon^{aa}, M-L. Turluer^{an}, I.A. Tyapkin^p, P. Tyapkin^x,
S. Tzamarias^k, O. Ullalandⁱ, V. Uvarov^{aq}, G. Valenti^{ie}, E. Vallazza^{au},
C. Vander Velde^b, P. Van Dam^{ae}, W. Van den Boeck^b, J. Van Eldik^{iae},
A. Van Lysebetten^b, N. van Remortel^b, I. Van Vulpen^{ae}, G. Vegni^{aa}, L. Ventura^{aj},
W. Venus^{ak,i}, F. Verbeure^b, P. Verdier^y, M. Verlato^{aj}, L.S. Vertogradov^p,
V. Verzi^{aa}, D. Vilanova^{an}, L. Vitale^{au}, E. Vlasov^{aq}, A.S. Vodopyanov^p,
G. Voulgaris^c, V. Vrba^l, H. Wahlen^{ba}, A.J. Washbrook^v, C. Weiserⁱ,
D. Wickeⁱ, J.H. Wickens^b, G.R. Wilkinson^{ai}, M. Winter^j, M. Witek^r,
G. Wolfⁱ, J. Yi^a, O. Yushchenko^{aq}, A. Zalewska^r, P. Zalewski^{az},
D. Zavrtnik^{ar}, E. Zevgolatakos^k, N.I. Zimin^{p,x}, A. Zintchenko^p,
Ph. Zoller^j, G. Zumerle^{aj}, M. Zupan^k

^a Department of Physics and Astronomy, Iowa State University, Ames IA 50011-3160, USA

^b Physics Department, Univ. Instelling Antwerpen, Universiteitsplein 1, B-2610 Antwerpen, Belgium,
and IIHE, ULB-VUB, Pleinlaan 2, B-1050 Brussels, Belgium,

and Faculté des Sciences, Univ. de l'Etat Mons, Av. Maistriau 19, B-7000 Mons, Belgium

^c Physics Laboratory, University of Athens, Solonos Str. 104, GR-10680 Athens, Greece

^d Department of Physics, University of Bergen, Allégaten 55, NO-5007 Bergen, Norway

- ^c Dipartimento di Fisica, Università di Bologna and INFN, Via Irnerio 46, IT-40126 Bologna, Italy
- ^f Centro Brasileiro de Pesquisas Físicas, rua Xavier Sigaud 150, BR-22290 Rio de Janeiro, Brazil, and Depto. de Física, Pont. Univ. Católica, C.P. 38071 BR-22453 Rio de Janeiro, Brazil, and Inst. de Física, Univ. Estadual do Rio de Janeiro, rua São Francisco Xavier 524, Rio de Janeiro, Brazil
- ^g Comenius University, Faculty of Mathematics and Physics, Mlynska Dolina, SK-84215 Bratislava, Slovakia
- ^h Collège de France, Lab. de Physique Corpusculaire, IN2P3-CNRS, FR-75231 Paris Cedex 05, France
- ⁱ CERN, CH-1211 Geneva 23, Switzerland
- ^j Institut de Recherches Subatomiques, IN2P3 - CNRS / ULP - BP20, FR-67037 Strasbourg Cedex, France
- ^k Institute of Nuclear Physics, N.C.S.R. Demokritos, P.O. Box 60228, GR-15310 Athens, Greece
- ^l FZU, Inst. of Phys. of the C.A.S. High Energy Physics Division, Na Slovance 2, CZ-180 40, Praha 8, Czech Republic
- ^m Dipartimento di Fisica, Università di Genova and INFN, Via Dodecaneso 33, IT-16146 Genova, Italy
- ⁿ Institut des Sciences Nucléaires, IN2P3-CNRS, Université de Grenoble 1, FR-38026 Grenoble Cedex, France
- ^o Helsinki Institute of Physics, HIP, P.O. Box 9, FI-00014 Helsinki, Finland
- ^p Joint Institute for Nuclear Research, Dubna, Head Post Office, P.O. Box 79, RU-101 000 Moscow, Russian Federation
- ^q Institut für Experimentelle Kernphysik, Universität Karlsruhe, Postfach 6980, DE-76128 Karlsruhe, Germany
- ^r Institute of Nuclear Physics and University of Mining and Metalurgy, Ul. Kawiorów 26a, PL-30055 Krakow, Poland
- ^s Université de Paris-Sud, Lab. de l'Accélérateur Linéaire, IN2P3-CNRS, Bât. 200, FR-91405 Orsay Cedex, France
- ^t School of Physics and Chemistry, University of Lancaster, Lancaster LA1 4YB, UK
- ^u LIP, IST, FCUL - Av. Elias Garcia, 14-1º, PT-1000 Lisboa Codex, Portugal
- ^v Department of Physics, University of Liverpool, P.O. Box 147, Liverpool L69 3BX, UK
- ^w LPNHE, IN2P3-CNRS, Univ. Paris VI et VII, Tour 33 (RdC), 4 place Jussieu, FR-75252 Paris Cedex 05, France
- ^x Department of Physics, University of Lund, Sölvegatan 14, SE-223 63 Lund, Sweden
- ^y Université Claude Bernard de Lyon, IPNL, IN2P3-CNRS, FR-69622 Villeurbanne Cedex, France
- ^z Univ. d'Aix - Marseille II - CPP, IN2P3-CNRS, FR-13288 Marseille Cedex 09, France
- ^{aa} Dipartimento di Fisica, Università di Milano and INFN-MILANO, Via Celoria 16, IT-20133 Milan, Italy
- ^{ab} Dipartimento di Fisica, Univ. di Milano-Bicocca and INFN-MILANO, Piazza delle Scienze 2, IT-20126 Milan, Italy
- ^{ac} Niels Bohr Institute, Blegdamsvej 17, DK-2100 Copenhagen Ø, Denmark
- ^{ad} IPNP of MFF, Charles Univ., Areal MFF, V Holesovickach 2, CZ-180 00, Praha 8, Czech Republic
- ^{ae} NIKHEF, Postbus 41882, NL-1009 DB Amsterdam, The Netherlands
- ^{af} National Technical University, Physics Department, Zografou Campus, GR-15773 Athens, Greece
- ^{ag} Physics Department, University of Oslo, Blindern, NO-1000 Oslo 3, Norway
- ^{ah} Dpto. Física, Univ. Oviedo, Avda. Calvo Sotelo s/n, ES-33007 Oviedo, Spain
- ^{ai} Department of Physics, University of Oxford, Keble Road, Oxford OX1 3RH, UK
- ^{aj} Dipartimento di Fisica, Università di Padova and INFN, Via Marzolo 8, IT-35131 Padua, Italy
- ^{ak} Rutherford Appleton Laboratory, Chilton, Didcot OX11 0QX, UK
- ^{al} Dipartimento di Fisica, Università di Roma II and INFN, Tor Vergata, IT-00173 Rome, Italy
- ^{am} Dipartimento di Fisica, Università di Roma III and INFN, Via della Vasca Navale 84, IT-00146 Rome, Italy
- ^{an} DAPNIA / Service de Physique des Particules, CEA-Saclay, FR-91191 Gif-sur-Yvette Cedex, France
- ^{ao} Institut de Física de Cantabria (CSIC-UC), Avda. los Castros s/n, ES-39006 Santander, Spain
- ^{ap} Dipartimento di Fisica, Università degli Studi di Roma La Sapienza, Piazzale Aldo Moro 2, IT-00185 Rome, Italy
- ^{aq} Inst. for High Energy Physics, Serpukov P.O. Box 35, Protvino (Moscow Region), Russian Federation
- ^{at} J. Stefan Institute, Jamova 39, SI-1000 Ljubljana, Slovenia
- and Laboratory for Astroparticle Physics, Nova Gorica Polytechnic, Kostanjevska 16a, SI-5000 Nova Gorica, Slovenia, and Department of Physics, University of Ljubljana, SI-1000 Ljubljana, Slovenia
- ^{as} Fysikum, Stockholm University, Box 6730, SE-113 85 Stockholm, Sweden
- ^{at} Dipartimento di Fisica Sperimentale, Università di Torino and INFN, Via P. Giuria 1, IT-10125 Turin, Italy
- ^{au} Dipartimento di Fisica, Università di Trieste and INFN, Via A. Valerio 2, IT-34127 Trieste, Italy, and Istituto di Fisica, Università di Udine, IT-33100 Udine, Italy
- ^{av} Univ. Federal do Rio de Janeiro, C.P. 68528 Cidade Univ., Ilha do Fundão, BR-21945-970 Rio de Janeiro, Brazil
- ^{aw} Department of Radiation Sciences, University of Uppsala, P.O. Box 535, SE-751 21 Uppsala, Sweden
- ^{ax} IFIC, Valencia-CSIC, and D.F.A.M.N., U. de Valencia, Avda. Dr. Moliner 50, ES-46100 Burjassot (Valencia), Spain
- ^{ay} Institut für Hochenergiephysik, Österr. Akad. d. Wissensch., Nikolsdorfergasse 18, AT-1050 Vienna, Austria
- ^{az} Inst. Nuclear Studies and University of Warsaw, Ul. Hoza 69, PL-00681 Warsaw, Poland
- ^{ba} Fachbereich Physik, University of Wuppertal, Postfach 100 127, DE-42097 Wuppertal, Germany

Received 13 July 2000; accepted 24 July 2000

Editor: L. Montanet

Abstract

Searches for charginos, neutralinos and sleptons at LEP2 centre-of-mass energies from 130 GeV to 189 GeV have been used to set lower limits on the mass of the Lightest Supersymmetric Particle and other supersymmetric particles within the MSSM framework. R-parity conservation has been assumed. The lightest neutralino was found to be heavier than $32.3 \text{ GeV}/c^2$ independent of the m_0 value. The lightest chargino, the second-to-lightest neutralino, the next-to-heaviest neutralino, the heaviest neutralino, the sneutrino and the right-handed selectron were found to be heavier than $62.4 \text{ GeV}/c^2$, $62.4 \text{ GeV}/c^2$, $99.9 \text{ GeV}/c^2$, $116.0 \text{ GeV}/c^2$, $61.0 \text{ GeV}/c^2$, and $87.0 \text{ GeV}/c^2$, respectively. These limits do not depend on m_0 or M_2 and are valid for $1 \leq \tan\beta \leq 40$, in the μ region where the lightest neutralino is the LSP. If the sneutrino is heavier than the chargino the lightest neutralino has to be heavier than $32.4 \text{ GeV}/c^2$. The effects of mixings in the third family of sfermions on these limits are discussed. The confidence level of all limits given is 95%. © 2000 Published by Elsevier Science B.V.

1. Introduction

In 1998 the LEP centre-of-mass energy reached 188.7 GeV and the DELPHI experiment collected an integrated luminosity of 158 pb^{-1} . These data have been analysed to search for the sfermions, charginos and neutralinos predicted by supersymmetric (SUSY) models [1].

In this paper we interpret the results of the DELPHI searches presented in Refs. [2–11] to constrain the masses of the following supersymmetric particles: the lightest neutralino ($\tilde{\chi}_1^0$), the lightest chargino ($\tilde{\chi}_1^\pm$), the heavier neutralinos ($\tilde{\chi}_2^0, \tilde{\chi}_3^0, \tilde{\chi}_4^0$), the sneutrino ($\tilde{\nu}$), and the selectron (\tilde{e}). The lightest neutralino is assumed to be the Lightest Supersymmetric Particle (LSP). The conservation of R-parity, implying a stable LSP, is also assumed. The stable neutralino is a good dark matter candidate and its mass is of importance in cosmology.

The Minimal Supersymmetric Standard Model (MSSM) scheme with gravity mediated supersymmetry breaking and with universal parameters at the high mass scale typical of Grand Unified Theories (GUT's) is assumed [1]. The parameters of this model relevant to the present analysis are the masses M_1 and M_2 of the gaugino sector (which are assumed to satisfy the GUT relation $M_1 = \frac{5}{3}\tan^2\theta_w M_2 \approx 0.5M_2$ at the electroweak scale), the universal mass parameter m_0 of the sfermion sector, the trilinear

couplings A_τ, A_b, A_t , determining the mass mixing in the third family of sfermions, the Higgs mass parameter μ , and the ratio $\tan\beta$ of the vacuum expectation values of the two Higgs doublets. The model assumed here is slightly more general than the minimal Super Gravity (mSUGRA) scenario: no general unification of scalar masses was assumed and, as a consequence, the Electroweak Symmetry breaking condition was not used to determine the absolute value of μ . No assumption about unification of trilinear couplings at the GUT scale was made either.

The mass spectrum of the charginos and neutralinos, and the LSP mass in particular, depend on the three parameters: M_2 (which is traditionally taken as the free parameter), μ , and $\tan\beta$ (see Fig. 1 for an example of isomass contours of $\tilde{\chi}_1^0$ and $\tilde{\chi}_1^\pm$ in the (μ, M_2) plane for two values of $\tan\beta$). If the sfermions are heavy, the decays of the $\tilde{\chi}_1^\pm$ and the $\tilde{\chi}_2^0$ proceed predominantly via W and Z respectively. This leads to $q\bar{q}\tilde{\chi}_1^0$ or $l\nu\tilde{\chi}_1^0$ final states in the case of chargino decay, and to $q\bar{q}\tilde{\chi}_1^0$ or $l^+l^-\tilde{\chi}_1^0$ states for $\tilde{\chi}_2^0$ decays.

If the sfermions are heavy, chargino production is the most important SUSY detection channel for large regions in the parameter space. However, if the sneutrino is light (below about $300 \text{ GeV}/c^2$) and the SUSY parameters take particular values [12], the chargino production cross-section at a given energy can be greatly reduced by destructive interference between the s -channel (Z/γ) and t -channel ($\tilde{\nu}$) contributions. On the other hand, if the selectron is light, the neutralino production cross-section is en-

E-mail address: Clara.Matteuzzi@cern.ch (C. Matteuzzi).

¹ Now at DESY-Zeuthen, Platanenallee 6, D-15735 Zeuthen, Germany.

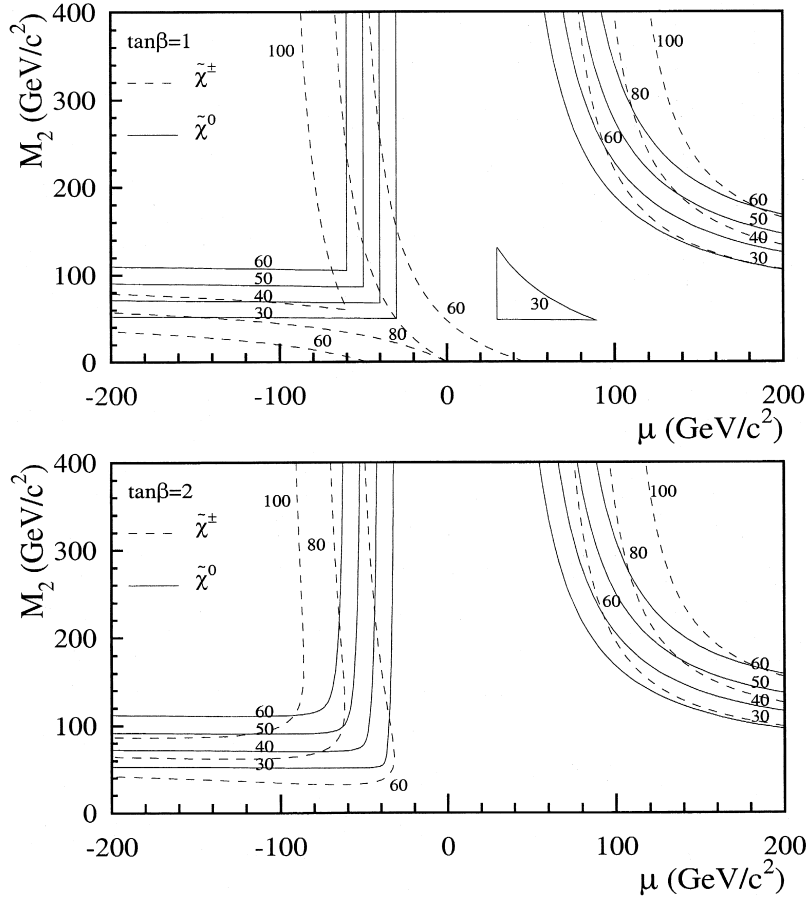


Fig. 1. An example of isomass contours in the (μ, M_2) plane for $\tilde{\chi}_1^0$ (solid lines) and $\tilde{\chi}_1^\pm$ (dashed lines) for $\tan\beta = 1$ (the upper plot) and $\tan\beta = 2$ (the lower plot). The chargino and neutralino mass formulae are invariant under the exchange $\tan\beta \leftrightarrow \cot\beta$, so the isomass contours for $\tan\beta = 0.5$ look like those for $\tan\beta = 2$. The value of $\Delta M = M_{\tilde{\chi}_1^\pm} - M_{\tilde{\chi}_1^0}$ tends to zero for large M_2 (higgsino region) and to $M_{\tilde{\chi}_1^\pm}/2$ for large $|\mu|$ (gaugino region). The value of $M_{\tilde{\chi}_2^0}$ (not shown here) tends to $M_{\tilde{\chi}_1^\pm}$ both for large M_2 and large $|\mu|$. These features do not depend on $\tan\beta$.

hanced due to t -channel selectron exchange (\tilde{e}_L, \tilde{e}_R) [13].

If the sfermions are light enough, chargino and neutralino decays can produce them and the decay branching ratios then depend on the sfermion masses, which in turn depend on m_0 in addition to M_2 and $\tan\beta$. In the third sfermion family, mixing between left and right sfermions may occur. For large $|\mu|$ this can give light stau and sbottom (\tilde{b}) states for large $\tan\beta$, and light stop (\tilde{t}) states for small $\tan\beta$.

The sensitivity of searches for sparticle production depends on the visible energy released in the decay process, which in turn depends primarily on

the mass difference between the decaying sparticle and an undetectable sparticle emitted in the process. If the sfermions are heavy, a particular situation arises at a very large M_2 , when both $M_{\tilde{\chi}_1^\pm} - M_{\tilde{\chi}_1^0}$ and $M_{\tilde{\chi}_2^0} - M_{\tilde{\chi}_1^0}$ tend to be small, causing a decrease in the search sensitivity. For light sleptons the chargino decay modes a) $\tilde{\chi}_1^\pm \rightarrow \tilde{\nu} \ell$, or b) $\tilde{\chi}_1^\pm \rightarrow \tilde{\tau} \nu$ with $\tilde{\tau} \rightarrow \tilde{\chi}_1^0 \tau$ could be present. In such cases chargino pair production could be hard to detect if $M_{\tilde{\chi}_1^\pm} - M_{\tilde{\nu}}$ or $M_{\tilde{\tau}} - M_{\tilde{\chi}_1^0}$ were small.

As no general unification of scalar masses was assumed, the mass spectrum of the Higgs sector, and thus the decay branching ratios of heavier neutrali-

nos ($\tilde{\chi}_2^0, \tilde{\chi}_3^0, \tilde{\chi}_4^0$), depends on one more parameter, which is taken to be the pseudoscalar Higgs mass, M_A . This mass was assumed to be 300 GeV/ c^2 , but the results depend only weakly on this assumption. The results of the Higgs boson searches at $\sqrt{s} = 189$ GeV [14,15] are not used in the present paper because, as we illustrate below, they have little impact.

2. The method

The method employed to set a lower limit on the LSP mass and on the masses of other supersymmetric particles is to convert the negative results of searches for charginos, neutralinos and sleptons into exclusion regions in the (μ, M_2) plane for different $\tan\beta$ values, and then to find the minimal allowed sparticle masses as a function of $\tan\beta$. Unless stated otherwise, the limits presented in this letter are valid for any M_2 and for the μ region in which the lightest neutralino is the LSP. The μ range depends on the values of $\tan\beta$ and m_0 , and on the mixing parameters in the third family (A_τ, A_t, A_b). Unless stated otherwise, for high values of m_0 (above 500 GeV/ c^2) the μ range between -2000 and 2000 GeV/ c^2 was scanned, but the scan range was increased if any limit point was found to be close to the scan boundary.

In the rest of this section we summarize briefly the methods employed and the results achieved in the searches for charginos, neutralinos and sleptons (subsection 2.1), and we present the method of combining different searches (subsection 2.2).

2.1. Searches for sleptons, neutralinos and charginos

Searches for sleptons. The results [2] of the DELPHI slepton search at 189 GeV were used. For smuon and selectron production, in addition to the typical decay mode $\tilde{\ell} \rightarrow \tilde{\chi}_1^0 \ell$, the cascade decay $\tilde{\ell} \rightarrow \tilde{\chi}_2^0 \ell$ with $\tilde{\chi}_2^0 \rightarrow \gamma \tilde{\chi}_1^0$ was also searched for. This decay is important for low $|\mu|$. These searches exclude slepton pair production with a cross-section above (0.05–0.2) pb depending on the neutralino mass and on the slepton mass, and assuming 100% branching fraction to the above decay modes.

Searches for neutralinos. The searches for neutralino production are described in Refs. [3–7]. They cover a variety of final state topologies which are important for setting the limit on the LSP mass. The topologies with two acoplanar (with the beam) jets, leptons or photons, and the multilepton, multijet, multijet with photons, single photon, and single tau topologies have all been searched for. They arise from $\tilde{\chi}_k^0 \tilde{\chi}_j^0$ final states with cascade and direct decays of heavier neutralinos: $\tilde{\chi}_k^0(\tilde{\chi}_j^0) \rightarrow \tilde{\chi}_i^0 + f\bar{f}$ or $\tilde{\chi}_k^0(\tilde{\chi}_j^0) \rightarrow \tilde{\chi}_i^0 + \gamma$ ($k = 2,3,4; j, i = 1,2,3$). The latter decay channel is enhanced in the region of small M_2 and $\mu < 0$ for $\tan\beta = 1$ and, even at high m_0 , extends the exclusion beyond the kinematic limit for chargino production [6]. The cross-section limits are typically around (0.2–0.4) pb. The search for neutralino production is sensitive to the particular kinematic configurations when neutralinos decay via light stau states and M_τ is close to $M_{\tilde{\chi}_1^0}$: the production of $\tilde{\chi}_1^0 \tilde{\chi}_2^0$ [6] with $\tilde{\chi}_2^0 \rightarrow \tilde{\tau}\tau$ and $\tilde{\tau} \rightarrow \tilde{\chi}_1^0 \tau$ leads to only one τ visible in the detector in this case, but nevertheless limits on the cross-section times branching ratio are of the order of 0.25 pb.

Searches for charginos. The searches in DELPHI [4,5,8,9] for pair-production of charginos which subsequently decay via $\tilde{\chi}_1^\pm \rightarrow \tilde{\chi}_1^0 W^*$ and $\tilde{\chi}_1^\pm \rightarrow \tilde{\chi}_2^0 W^* \rightarrow \tilde{\chi}_1^0 \gamma W^*$ exclude chargino pair production with cross-section larger than 0.13 pb if $\Delta M > 20$ GeV/ c^2 [9], where $\Delta M = M_{\tilde{\chi}_1^\pm} - M_{\tilde{\chi}_1^0}$. The search presented in [9] is sensitive down to $\Delta M = 3$ GeV/ c^2 , while the region of lower ΔM is covered by the search for $\tilde{\chi}_1^\pm \tilde{\chi}_1^\pm \gamma$ production (3 GeV/ $c^2 > \Delta M > 0.170$ GeV/ c^2), with the γ arising from initial state radiation, and by the search for stable heavy particles and long lived heavy particles (0.170 GeV/ $c^2 > \Delta M$) [10].

2.2. Combination of different searches

In the scan of the SUSY parameter space two approaches were adopted. In the first approach the efficiencies of the different searches, as obtained in Refs. [2–11] by DELPHI, were parametrised for the dominant channels, and used together with the information about the numbers of events selected in the data and the expected numbers of background events. The 95 % confidence level exclusion regions obtained with the different searches were then simply superimposed.

In a parallel approach, these searches were combined using a very fast detector simulation program (SGV) [6], together with SUSYGEN [16], to simulate simultaneously all channels of chargino, neutralino, slepton and squark production and decay. This was done for about 500000 SUSY points. The selection criteria of the neutralino searches [6] could then be applied directly. The results obtained with different neutralino topologies were combined using the multichannel Bayesian approach [17].

Good agreement was found between the two approaches, when the same channels were used. In particular, the efficiencies obtained with the very fast simulation were found to agree well with the full simulation results [6]. However, because the efficiencies were parametrised only for the dominant channels, the results obtained using parametrised efficiencies were found to be too conservative. The results of the fast simulation scan were therefore used in the regions of the parameter space where decay channels different from the ones the various searches were originally designed for were found to be important², or where several SUSY production processes contributed and the searches for them would otherwise not be efficiently combined. The combined exclusion in each MSSM point is in this case obtained by directly applying the selection criteria to all processes which should occur in this particular point.

The typical scan step size in μ and M_2 was 1 GeV/ c^2 except in the region of the LSP limit, where the step size was decreased to 0.05 GeV/ c^2 . The step size in m_0 was varying, the density of points being increased in regions of potentially difficult mass configurations. Special care was taken to set up the scan logic in such a way that no such configuration was overlooked. In particular, whenever two nearby scan points were excluded by different searches, the scan was performed with smaller steps between these points to check the continuity of the exclusion.

² The search for neutralinos covers many topologies typical of SUSY particle production. For example, they are relevant in the search for the selectron production as well. In particular, when the cascade decays of the selectron are important, namely $\tilde{e} \rightarrow \tilde{\chi}_2^0 e$ with $\tilde{\chi}_2^0 \rightarrow q\bar{q}\tilde{\chi}_1^0$ or $\tilde{\chi}_2^0 \rightarrow \ell\bar{\ell}\tilde{\chi}_1^0$, the standard search for selectron production is not efficient.

3. Results

The unification of sfermion masses to a common m_0 at the GUT scale allows sfermion masses at the Electroweak Scale to be calculated as functions of $\tan\beta$, M_2 and m_0 . In particular the sneutrino ($\tilde{\nu}$), the left-handed selectron and smuon ($\tilde{e}_L, \tilde{\mu}_L$) and the right-handed selectron and smuon ($\tilde{e}_R, \tilde{\mu}_R$) masses can be expressed as³:

- 1) $M_{\tilde{\nu}}^2 = m_0^2 + 0.77M_2^2 + 0.5M_Z^2\cos 2\beta$
- 2) $M_L^2 = m_0^2 + 0.77M_2^2 - 0.27M_Z^2\cos 2\beta$
- 3) $M_R^2 = m_0^2 + 0.22M_2^2 - 0.23M_Z^2\cos 2\beta$

In the high m_0 scenario, $m_0 = 1000$ GeV/ c^2 was assumed, which implied sfermion masses of the same order. Limits arise in this case from a combination of the chargino and neutralino searches described in [9,10] and [6].

For high m_0 , the chargino pair-production cross-section is large and the chargino is excluded nearly up to the kinematic limit, provided $M_2 < 200$ GeV/ c^2 . As already mentioned, a particular situation arises for very high values of M_2 , where $\Delta M = M_{\tilde{\chi}_1^\pm} - M_{\tilde{\chi}_1^0}$ is small. However the search presented in [9] is sensitive down to $\Delta M = 3$ GeV/ c^2 , which occurs for $M_2 \approx 1400$ GeV/ c^2 , and the region of $M_2 > 1400$ GeV/ c^2 is covered by the chargino searches described in [10]. The limits presented here are thus valid for any M_2 .

It may also be remarked that at low M_2 , $\Delta M = M_{\tilde{\chi}_1^\pm} - M_{\tilde{\chi}_1^0}$ is large, resulting in increased background from W^+W^- production. However, if $|\mu|$ is low as well, the chargino tends to decay via $\tilde{\chi}_1^\pm \rightarrow \tilde{\chi}_2^0 W^*$ to the next-to-lightest neutralino $\tilde{\chi}_2^0$, which then decays by $\tilde{\chi}_2^0 \rightarrow \tilde{\chi}_1^0 \gamma$ or $\tilde{\chi}_2^0 \rightarrow \tilde{\chi}_1^0 Z^*$. For setting the limit on the LSP mass, it is therefore important that the chargino search includes topologies with photons stemming from the decays $\tilde{\chi}_1^\pm \rightarrow \tilde{\chi}_2^0 W^* \rightarrow \tilde{\chi}_1^0 \gamma W^*$, since the search for topologies with photons does not suffer from W^+W^- background and is effective for large ΔM (close to M_W).

Of the detectable neutralino production channels (i.e. excluding $\tilde{\chi}_1^0 \tilde{\chi}_1^0$), the $\tilde{\chi}_1^0 \tilde{\chi}_2^0$ and $\tilde{\chi}_1^0 \tilde{\chi}_3^0$ channels are important for large regions in the parameter

³ It is worth noting that for $\tan\beta \geq 1$ ($\tan\beta < 1$) we have $\cos 2\beta \leq 0$ ($\cos 2\beta > 0$), so the $\tilde{\nu}$ is never heavier (lighter) than the \tilde{e}_L .

space, but in order to cover as much as possible one must also consider channels like $\tilde{\chi}_2^0 \tilde{\chi}_3^0$ and $\tilde{\chi}_2^0 \tilde{\chi}_4^0$, giving cascade decays with multiple jets or leptons in the final state. At high m_0 the production cross-

section for all these neutralino production channels drops to very low values for $|\mu|$ above ≈ 75 GeV/c^2 . This is because the two lightest neutralinos then have large photino ($\tilde{\chi}_1^0$) and zino ($\tilde{\chi}_2^0$) compo-

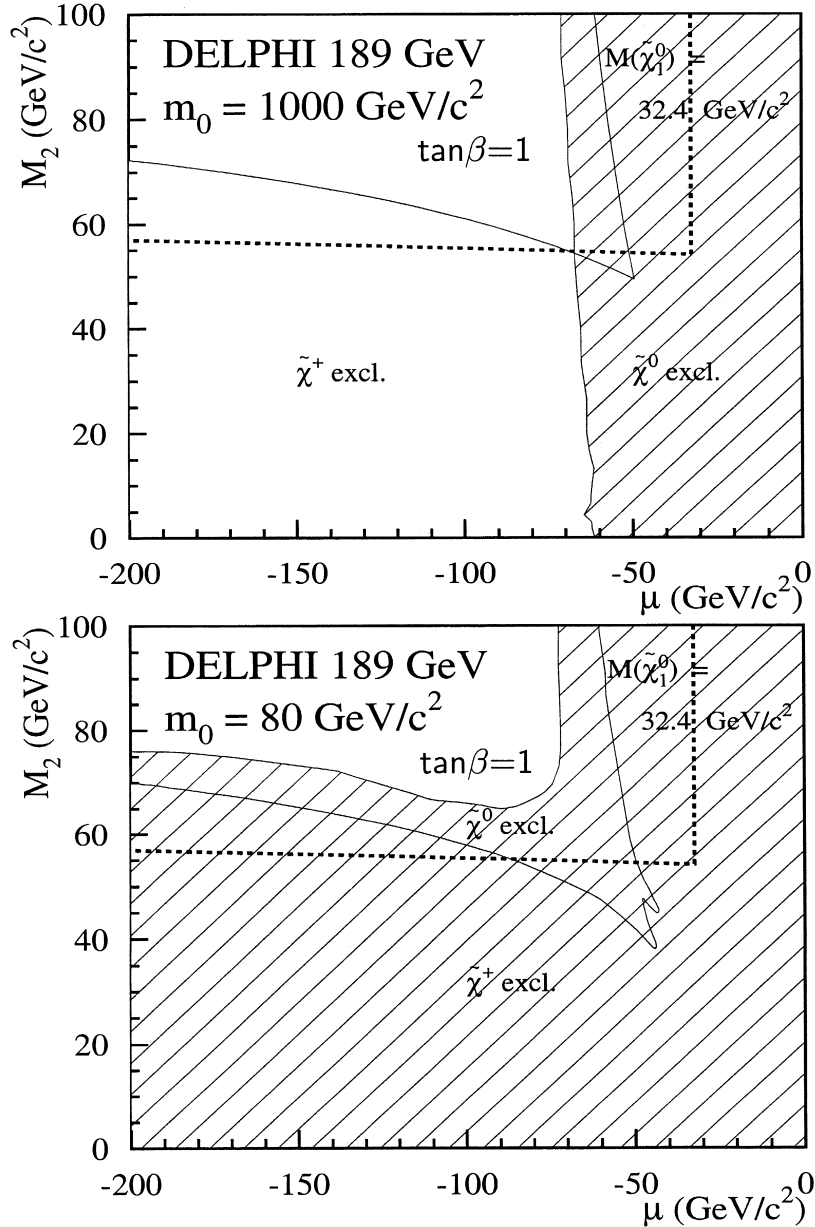


Fig. 2. Excluded regions in the (μ, M_2) plane for $\tan\beta = 1$ for $m_0 = 1000 \text{ GeV}/c^2$ (upper plot) and $m_0 = 80 \text{ GeV}/c^2$ (lower plot). The shaded areas show regions excluded by searches for charginos and the hatched areas show regions excluded by searches for neutralinos. The thick dashed curve shows the isomass contour for $M_{\tilde{\chi}_1^0} = 32.4 \text{ GeV}/c^2$, the lower limit on the LSP mass obtained at $\tan\beta = 1$. The chargino exclusion in the upper plot is close to the isomass contour for $M_{\tilde{\chi}_1^\pm}$ at the kinematic limit (upper plot in Fig. 1).

nents and their s -channel pair-production is therefore suppressed, while pair-production of heavier neutralinos is not kinematically accessible. Nevertheless, for $\tan\beta < 1.2$ and $M_2 > 60 \text{ GeV}/c^2$ the neutralino exclusion reaches beyond the kinematic limit for chargino production at negative μ (see Fig. 2 and [6]). This region is important for setting the limit on the LSP mass.

For medium m_0 , $100 \text{ GeV}/c^2 \lesssim m_0 \lesssim 1000 \text{ GeV}/c^2$, the $\tilde{\chi}_1^0 \tilde{\chi}_2^0$ production cross-section in the gaugino-region ($|\mu| \gtrsim 75 \text{ GeV}/c^2$) grows quickly as m_0 falls, due to the rapidly rising contribution from the selectron t -channel exchange. Meanwhile the chargino production cross-section in the gaugino region drops slowly, but it remains high enough to allow chargino exclusion nearly up to the kinematic limit for $m_0 \gtrsim 200 \text{ GeV}/c^2$. For lower $m_0 \sim 100 \text{ GeV}/c^2$, the chargino production cross-section

in the gaugino region is close to its minimum, while the neutralino production cross-section is very much enhanced. Consequently the region of the (μ, M_2) parameter space excluded by searches for neutralino production at low m_0 is larger than the one excluded by the search for chargino and neutralino production at high m_0 (see Fig. 2 and [6]).

For low m_0 , $m_0 \lesssim 100 \text{ GeV}/c^2$, and low M_2 , $M_2 \lesssim 200 \text{ GeV}/c^2$, the situation is much more complicated because light sfermions affect not only the production cross-sections but also the decay patterns of charginos and neutralinos. They can also be searched for in direct pair-production. Exclusion regions at low m_0 arise from the combination of searches for chargino, neutralino and slepton production.

For low m_0 and M_2 the sneutrino is light, and for $M_{\tilde{\chi}_1^\pm} > m_{\tilde{\nu}}$ the chargino decay mode $\tilde{\chi}_1^\pm \rightarrow \tilde{\nu} \ell$ is

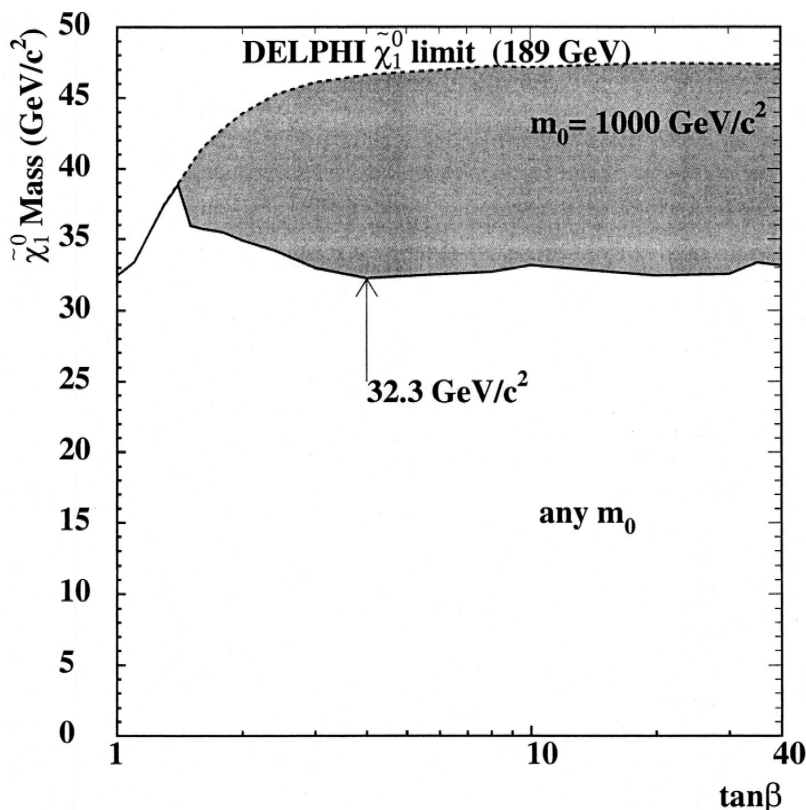


Fig. 3. The lower limit at 95 % confidence level on the mass of the lightest neutralino, $\tilde{\chi}_1^0$, as a function of $\tan\beta$ assuming a stable $\tilde{\chi}_1^0$. The dashed curve shows the limit obtained for $m_0 = 1000 \text{ GeV}/c^2$, the solid curve shows the limit obtained allowing for any m_0 .

dominant, leading to an experimentally undetectable final state if $M_{\tilde{\chi}_1^\pm} \simeq m_{\tilde{\nu}}$. In the gaugino region, for every value of M_2 and μ , an m_0 can be found such that $M_{\tilde{\chi}_1^\pm} \simeq m_{\tilde{\nu}}$. The search for charginos cannot therefore be used to exclude regions in the (μ, M_2) plane if very low m_0 values are allowed. The search for selectron production is used instead to put a limit on the sneutrino mass (and thus on the chargino mass), the selectron and the sneutrino masses being related by relations 1)–3). The selectron pair production cross-section is typically larger than the smuon pair production cross-section, due to the contribution of t -channel neutralino exchange. However, at $|\mu| \lesssim 200 \text{ GeV}/c^2$ the selectron production cross-section tends to be small and the exclusion arises mainly from the search for neutralino pair-production.

Mixing between the left-handed and right-handed sfermion states can be important for the third family sfermions and lead to light $\tilde{\tau}_1$, \tilde{b}_1 and \tilde{t}_1 . Mass splitting terms at the Electroweak Scale proportional to $m_\tau(A_\tau - \mu \tan \beta)$, $m_b(A_b - \mu \tan \beta)$, and $m_t(A_t - \mu/\tan \beta)$ were considered for $\tilde{\tau}$, \tilde{b} , and \tilde{t} respectively. In the first instance $A_\tau = A_t = A_b = 0$ was assumed, then the dependence of the results on A_τ was studied. These terms lead to $\tilde{\tau}_1$, \tilde{b}_1 or \tilde{t}_1 being degenerate in mass with $\tilde{\chi}_1^0$ or being the LSP for large values of $|\mu|$. The results presented in this paper are limited to the range of the μ parameter where the lightest neutralino is the LSP.

For low $\tan \beta$ values (including $\tan \beta < 1$) it is first the stop and later the sbottom which become degenerate in mass with $\tilde{\chi}_1^{04}$. Neither stop-neutralino degeneracy nor sbottom-neutralino degeneracy introduces ‘blind spots’ in chargino detection, as $\tilde{\chi}_1^\pm \rightarrow \tilde{q}\tilde{q}$ remains visible. However, for $\tan \beta \geq 8$, the LSP mass limit occurs at high enough M_2 that $M_{\tilde{b}_1}$ is pushed above $M_{\tilde{\tau}_1}$ and $\tilde{\tau}_1$ can become degenerate in mass with $\tilde{\chi}_1^0$, while m_0 is high enough that selec-

tron and sneutrino pair-production are not allowed by kinematics. Chargino decay $\tilde{\chi}_1^\pm \rightarrow \tilde{\tau}\nu$ with $\tilde{\tau} \rightarrow \tilde{\chi}_1^0\tau$ is then hard to detect, leaving $\tilde{\chi}_1^0\tilde{\chi}_2^0$ and the $\tilde{\chi}_2^0\tilde{\chi}_2^0$ production with $\tilde{\chi}_2^0 \rightarrow \tilde{\tau}\tau$ as the only detectable sparticle production channels.

3.1. Results for high m_0

Fig. 3 gives the lower limit on $M_{\tilde{\chi}_1^0}$ as a function of $\tan \beta$. The lightest neutralino is constrained to have a mass:

$$M_{\tilde{\chi}_1^0} > 32.4 \text{ GeV}/c^2$$

for $m_0 = 1000 \text{ GeV}/c^2$ and any value of M_2 . The limit occurs at $\tan \beta = 1$. Fig. 2 (upper part) shows the region in the (μ, M_2) plane for $\tan \beta = 1$ excluded by the chargino and neutralino searches, relevant for the LSP mass limit at $m_0 = 1000 \text{ GeV}/c^2$. This result improves on the high m_0 one presented in [9] due to the constraint from the search for neutralino production. However, at $\tan \beta \geq 1.2$ the LSP limit is given exclusively by the chargino search and its value reaches about half of the limit on the chargino mass at high $\tan \beta$, where the iso-mass contours of $\tilde{\chi}_1^\pm$ and $\tilde{\chi}_1^0$ in the (μ, M_2) plane of Fig. 1 become parallel. The rise of the LSP limit for small $\tan \beta$ can be explained by the change of the shape of these contours with $\tan \beta$ (from Fig. 1 it can be seen that if, for example, $M_{\tilde{\chi}_1^\pm} \lesssim 100 \text{ GeV}/c^2$ was excluded, this would imply $M_{\tilde{\chi}_1^0} \gtrsim 35 \text{ GeV}/c^2$ for $\tan \beta = 1$ and $M_{\tilde{\chi}_1^0} \gtrsim 45 \text{ GeV}/c^2$ for $\tan \beta = 2$). It should be noted that, because the chargino and neutralino masses are invariant under exchange $\tan \beta \leftrightarrow 1/\tan \beta$, the point $\tan \beta = 1$ is the real minimum. The LSP limit for $\tan \beta < 1$ can be obtained by replacing $\tan \beta$ with $1/\tan \beta$ in Fig. 3.

The lowest non-excluded value of $M_{\tilde{\chi}_1^0}$ occurs for $\tan \beta = 1$, $\mu = -68.7 \text{ GeV}/c^2$ and $M_2 = 54.8 \text{ GeV}/c^2$. For these parameters, $\tilde{\chi}_4^0\tilde{\chi}_2^0$ production is kinematically allowed at $\sqrt{s} = 189 \text{ GeV}$ ($M_{\tilde{\chi}_4^0} = 118.9 \text{ GeV}/c^2$, $M_{\tilde{\chi}_2^0} = 68.7 \text{ GeV}/c^2$) and has a cross-section of 0.12 pb. The chargino pair-production cross-section is 0.11 pb. The cross-sections for the production of other gauginos are much smaller, and the limit arises from a combination of searches for $\tilde{\chi}_4^0\tilde{\chi}_2^0$ and $\tilde{\chi}_1^\pm\tilde{\chi}_1^\pm$ production. The dominant decays of $\tilde{\chi}_2^0$ are $\tilde{\chi}_2^0 \rightarrow q\bar{q}\tilde{\chi}_1^0$ (31%), $\tilde{\chi}_1^0\gamma$ (31%),

⁴The ‘mixing -independent’ (diagonal) terms of the mass matrices of squarks grow faster with M_2 than those of sleptons, and they have different dependence on $\tan \beta$. For example, for $A_t = A_\tau = A_b = 0$, $\mu = 0$, and $\tan \beta = 1$, both the \tilde{t}_1 and \tilde{b}_1 are heavier than the $\tilde{\tau}_1$; but they become lighter than the $\tilde{\tau}_1$ for large $|\mu|$ values. The mass hierarchy between $\tilde{\tau}_1$, \tilde{b}_1 , and \tilde{t}_1 depends on M_2 , $\tan \beta$, μ , and m_0 .

and $\nu\bar{\nu}\tilde{\chi}_1^0$ (15 %), and those of $\tilde{\chi}_4^0$ are $\tilde{\chi}_4^0 \rightarrow q\bar{q}\tilde{\chi}_2^0$ (56 %), $\nu\bar{\nu}\tilde{\chi}_2^0$ (17 %), and $h^0\tilde{\chi}_1^0$ (15.0 %)⁵.

Fig. 4 shows the lower limit on $M_{\tilde{\chi}_1^\pm}$ and $M_{\tilde{\chi}_1^0}$ as a function of M_2 for $\tan\beta = 1$. The upper part of the figure presents the limit on $M_{\tilde{\chi}_1^\pm}$ for $\mu < 0$: values of $M_{\tilde{\chi}_1^\pm}$ above the kinematic limit for chargino pair-production are excluded for $100 \text{ GeV}/c^2 < M_2 < 400 \text{ GeV}/c^2$ due to the constraint from the search for neutralino production. The lower part of the figure shows the limit on $M_{\tilde{\chi}_1^\pm}$ and $M_{\tilde{\chi}_1^0}$ for $-1000 \text{ GeV}/c^2 \leq \mu \leq 1000 \text{ GeV}/c^2$ and for M_2 up to $30\,000 \text{ GeV}/c^2$. For $M_2 > 1400 \text{ GeV}/c^2$ the limits are given by the results presented in [10]. The limit on the chargino mass for $m_0 = 1000 \text{ GeV}/c^2$ is:

$$M_{\tilde{\chi}_1^\pm} > 62.4 \text{ GeV}/c^2.$$

The limit does not depend on $\tan\beta$ and is valid for any M_2 . It occurs at very high M_2 values, where $M_{\tilde{\chi}_1^\pm}$, $M_{\tilde{\chi}_1^0}$ and $M_{\tilde{\chi}_2^0}$ are degenerate and $\Delta M = M_{\tilde{\chi}_1^\pm} - M_{\tilde{\chi}_1^0} \approx 0.170 \text{ GeV}/c^2$.

3.2. The LSP mass limit for any m_0

Fig. 3 gives the lower limit on $M_{\tilde{\chi}_1^0}$ as function of $\tan\beta$ for any m_0 . The ‘any m_0 ’ limit follows the high m_0 limit up to $\tan\beta = 1.2$ and then drops to its lowest value, $32.3 \text{ GeV}/c^2$, at $\tan\beta = 4$.

Thus

$$M_{\tilde{\chi}_1^0} > 32.3 \text{ GeV}/c^2$$

independent of m_0 . If the sneutrino is heavier than the chargino, the lowest non-excluded neutralino mass occurs at $\tan\beta = 1$, as above.

Fig. 5 illustrates the exclusion regions in the (μ, M_2) plane for $\tan\beta = 4$ near the ‘any m_0 ’ limit point, where both $\tilde{\chi}_1^\pm$ and $\tilde{\chi}_2^0$ are degenerate with the sneutrino ($m_0 = 71.2 \text{ GeV}/c^2$, $\mu = -277$

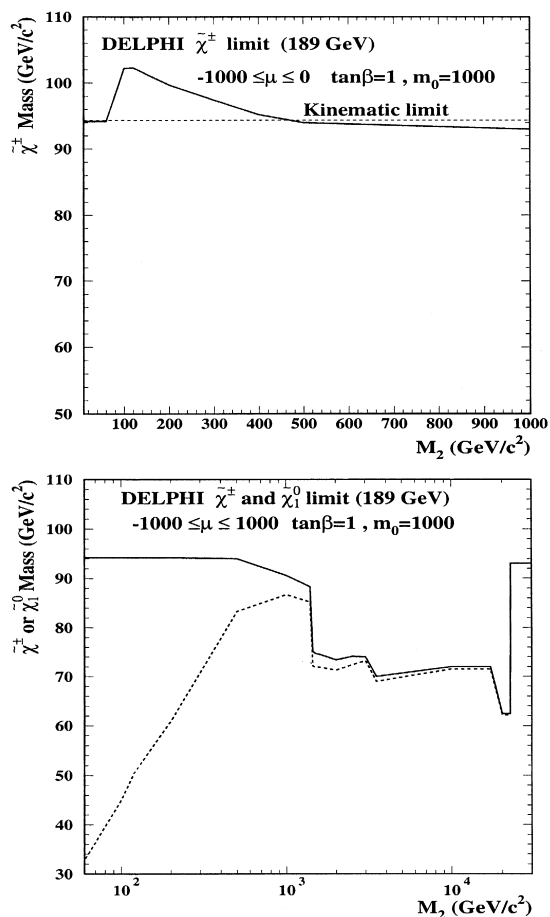


Fig. 4. Limits on $M_{\tilde{\chi}_1^\pm}$ and $M_{\tilde{\chi}_1^0}$ for $\tan\beta = 1$ and $m_0 = 1000 \text{ GeV}/c^2$ are shown as functions of M_2 . The upper figure shows the lower limit on $M_{\tilde{\chi}_1^\pm}$ (solid curve) for $-1000 \text{ GeV}/c^2 \leq \mu \leq 0$ resulting from searches for neutralinos and charginos. The dashed line shows the kinematic limit for chargino pair-production. The lower part of the figure shows the limit on $M_{\tilde{\chi}_1^\pm}$ (solid curve) and $M_{\tilde{\chi}_1^0}$ (dashed curve) for $-1000 \text{ GeV}/c^2 \leq \mu \leq 1000 \text{ GeV}/c^2$. The region of $M_2 < 55 \text{ GeV}/c^2$ is excluded (see Fig. 2).

GeV/c^2 , and $M_2 = 60.9 \text{ GeV}/c^2$, implying $M_{\tilde{\chi}_2^0} = 66.8 \text{ GeV}/c^2$, $M_{\tilde{\chi}_1^\pm} = 66.7 \text{ GeV}/c^2$, $M_{\tilde{\nu}} = 66 \text{ GeV}/c^2$, $M_{\tilde{e}_R} = 87.2 \text{ GeV}/c^2$, $M_{\tilde{\tau}_1} = 80.3 \text{ GeV}/c^2$, and $M_{h^0} = 87.4 \text{ GeV}/c^2$)⁶. The $M_{\tilde{\chi}_1^0} = 32.3 \text{ GeV}/c^2$ isomass curve is indicated. The exclusion

⁵ The $\tilde{\chi}_4^0$ branching fractions listed above correspond to $M_A = 300 \text{ GeV}/c^2$ and $A_t = 0$, which results in $M_{h^0} = 76 \text{ GeV}/c^2$. However, if $M_A = 1000 \text{ GeV}/c^2$ and $A_t = \mu/\tan\beta = \sqrt{6} \text{ TeV}/c^2$ (maximal M_{h^0} scenario used in [14]), M_{h^0} becomes $97 \text{ GeV}/c^2$ and the $h^0 Z$ production cross-section at $\sqrt{s} = 189 \text{ GeV}$ falls to 0.07 pb , so the point is no longer excluded by Higgs boson searches [14]. Searches for $\tilde{\chi}_4^0 \tilde{\chi}_2^0$ are not affected by the change of M_{h^0} from $76 \text{ GeV}/c^2$ to $97 \text{ GeV}/c^2$, as vanishing of the branching fraction $\tilde{\chi}_4^0 \rightarrow h^0 \tilde{\chi}_1^0$ is compensated by the increase of the $\tilde{\chi}_4^0 \rightarrow q\bar{q} \tilde{\chi}_2^0$ branching fractions and the change of the overall search efficiency is negligible.

⁶ M_{h^0} grows to $103 \text{ GeV}/c^2$ for the maximal allowed mixing; as before, the point is then no longer excluded by the Higgs boson searches [14].

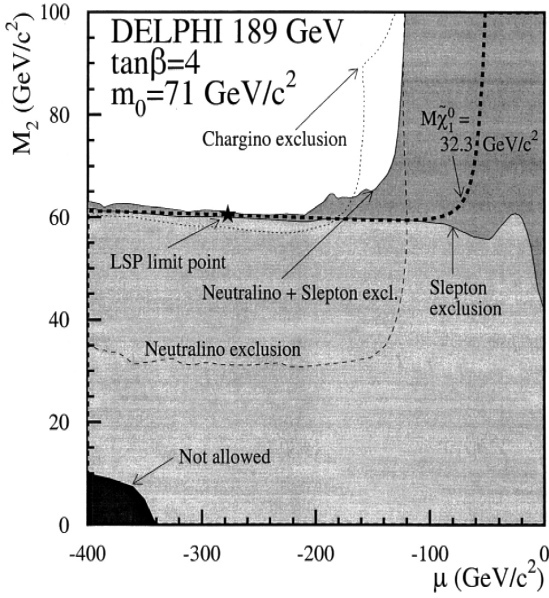


Fig. 5. Excluded regions in the (μ, M_2) plane for $m_0 = 71 \text{ GeV}/c^2$ and $\tan\beta = 4$. The thin curves show the regions excluded by searches for charginos (dotted) and neutralinos (dashed). The region excluded by the slepton search is shown in lighter shading and the thin solid curve. The combined neutralino-slepton exclusion is shown by the darker shading and the thin solid curve. The upper edge of the chargino exclusion for $\mu < -200 \text{ GeV}/c^2$ is determined by the upper edge of the combined neutralino-slepton exclusion. Also shown is the relevant isomass curve for $\tilde{\chi}_1^0$. The very dark shaded region is not allowed due to the stop being the LSP.

regions derived from searches for neutralino production, for slepton production and from the combined search for neutralino and slepton production are shown. The edge of the combined slepton and neutralino exclusion at $M_2 = 60.6 \text{ GeV}/c^2$ corresponds to the $M_{\tilde{e}_R} = 87.2 \text{ GeV}/c^2$ isomass curve. This edge imposes a limit on the sneutrino mass $M_{\tilde{\nu}} = 66 \text{ GeV}/c^2$, and determines the upper reach of the exclusion obtained from the search for the chargino production. As the various final state topologies which were used to search for neutralinos [6] (see subsection 2.1) were employed here also to search for slepton production (see subsection 2.2), the slepton exclusion does not deteriorate significantly for small negative values of μ where the $\tilde{\ell} \rightarrow \tilde{\chi}_2^0 \ell$ and $\tilde{\chi}_2^0 \rightarrow \ell^+ \ell^- \tilde{\chi}_1^0$ decay channels dominate, giving multilepton final states. This region is also covered

by the neutralino searches. However, for $M_2 > 30 \text{ GeV}/c^2$ and $\mu < -130 \text{ GeV}/c^2$ the invisible $\tilde{\chi}_2^0 \rightarrow \nu \tilde{\nu}$ branching fraction is above 90% and, because only $\tilde{\chi}_2^0 \tilde{\chi}_1^0$ and $\tilde{\chi}_2^0 \tilde{\chi}_2^0$ are produced in this region, the neutralino exclusion disappears.

3.2.1. The $\tan\beta$ dependence of the LSP mass limit

Fig. 6 shows the masses of the sneutrino, the \tilde{e}_R and the $\tilde{\tau}_1$ in the LSP limit points, as a function of $\tan\beta$. The $\tan\beta$ dependence of the LSP limit can be understood as follows.

For $\tan\beta < 1.2$, the (μ, M_2) region excluded by neutralino searches at low m_0 is larger than the region excluded by chargino and neutralino searches for large m_0 (see Fig. 2). Thus for $\tan\beta < 1.2$ the limit on the neutralino mass for ‘any m_0 ’ is given by the high m_0 limit of $32.4 \text{ GeV}/c^2$. The region in the (μ, M_2) plane excluded by neutralino searches at a given m_0 becomes smaller with the increase of $\tan\beta$ and the LSP mass limit is reached at a lower m_0 value.

At $\tan\beta \geq 1.4$ the minimal sneutrino mass allowed by the neutralino and slepton searches drops below $94 \text{ GeV}/c^2$ (see Fig. 6). This implies, as

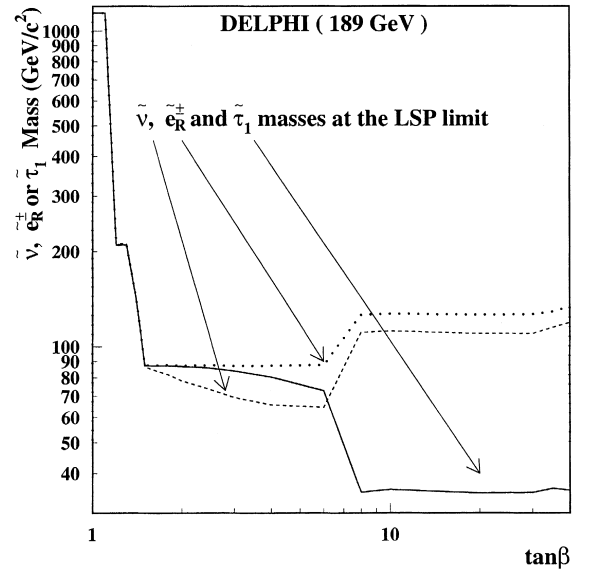


Fig. 6. The masses at the LSP limit point as a function of $\tan\beta$, of the sneutrino (dashed curve), \tilde{e}_R (dotted curve) and the lightest stau (solid curve). Mass splitting in the stau sector in the form $A_\tau - \mu \tan\beta$ was assumed, with $A_\tau = 0$.

explained above, that for $M_{\tilde{\chi}_1^\pm} < 94 \text{ GeV}/c^2$ an m_0 value can be found such that $M_{\tilde{\chi}_1^\pm} = m_{\tilde{\nu}}$ and the chargino decays ‘invisibly’. The limits are therefore given by the combination of searches for neutralino and slepton production.

For $4 \lesssim \tan\beta \lesssim 8$ the limit improves slightly due to the increase of the $\tilde{\tau}_1$ production cross-section, as $\tilde{\tau}_1$ gets lighter (see Fig. 6) when the mass splitting term ($A_\tau - \mu \tan\beta$) increases. For $\tan\beta > 6$ the $\tilde{\tau}_1$ pair production cross-section starts to be bigger than the $\tilde{\epsilon}_R \tilde{\epsilon}_R$ production cross-section in the $\mu < -200 \text{ GeV}/c^2$ region, where the chargino-sneutrino degeneracy occurs.

At $\tan\beta \gtrsim 8$ the limit degrades somewhat again due to the possibility of $M_{\tilde{\tau}_1}$ being close to $M_{\tilde{\chi}_1^0}$, which makes the $\tilde{\tau}_1$ undetectable. In this region the LSP limit is given by the neutralino exclusion, and reaches $M_{\tilde{\chi}_1^0} > 33.2 \text{ GeV}/c^2$ for⁷ $\tan\beta = 40$. The limit is reached for $m_0 = 122 \text{ GeV}/c^2$ and $\mu = -252.5 \text{ GeV}/c^2$, with $M_{\tilde{\tau}_1} = 35.4 \text{ GeV}/c^2$ and all other sleptons heavier than the kinematic limit for slepton pair-production⁸.

The LSP mass limit at $\tan\beta \leq 1$ can be obtained noting that, while the chargino and neutralino masses are invariant under $\tan\beta \leftrightarrow 1/\tan\beta$ exchange, the sign of the $\cos 2\beta$ term in relations 1)–3) changes, resulting in lighter selectrons and heavier sneutrinos for the same values of M_2 and m_0 . Thus, the selectron production cross-section, the chargino production cross-section and the neutralino production cross-section are all larger for the same M_2 , m_0 and μ values. The chargino-sneutrino degeneracy region is excluded at $\tan\beta < 1$, and the neutralino-stau degeneracy is not allowed. The LSP mass limit for $\tan\beta < 1$ is expected to rise with diminishing $\tan\beta$ to reach its high m_0 value when $1/\tan\beta$ is large.

⁷ The limit on the LSP mass obtained by the LEP SUSY working group [18] dropped to $30 \text{ GeV}/c^2$ at $\tan\beta = 35$ due to $M_{\tilde{\tau}_1}$ being close to $M_{\tilde{\chi}_1^0}$. This was because the search for neutralino production was not used in [18].

⁸ In this point the mass of the lightest Higgs boson is $M_{h^0} = 98 \text{ GeV}/c^2$, and h^0 decays nearly exclusively to $\tilde{\tau}_1 \tilde{\tau}_1$, thus ‘invisibly’. Present limits on h^0 decaying invisibly are $M_{h^0} > 95 \text{ GeV}/c^2$ [15], thus not sufficient for exclusion. Moreover, this point cannot be excluded from the measurement of the invisible Z width, due to the tiny $Z \rightarrow \tilde{\tau}_1 \tilde{\tau}_1$ coupling.

3.2.2. The dependence of the LSP limit on the mixing

The dependence of the LSP limit on the mixing in the stau sector was studied, while keeping $A_t = A_b = 0$. For A_τ large and positive, $\approx +1000 \text{ GeV}/c^2$, the limit at $\tan\beta = 4$ rises slightly due to the larger stau production cross-section. The limit for $\tan\beta \gtrsim 8$ falls because, with the larger splitting in the stau sector, the stau-neutralino mass degeneracy occurs for higher m_0 , where the neutralino production cross-section is lower. For A_τ large and negative, $\approx -1000 \text{ GeV}/c^2$, the range where the LSP limit occurs in the chargino-sneutrino degeneracy region extends to higher $\tan\beta$ values, as the $\tilde{\tau}_1$ is heavier for a smaller splitting. Finally, if there is no mass splitting in the $\tilde{\tau}$ sector, so that $A_\tau = \mu \tan\beta$, the limit degrades by $0.5 \text{ GeV}/c^2$. Overall, the dependence of the neutralino mass limit on the mixing in the stau sector is weak: the limit changes by $\leq 2 \text{ GeV}/c^2$ for a change of A_τ between $-1000 \text{ GeV}/c^2$ and $1000 \text{ GeV}/c^2$.

It should be noted that the A_τ values studied here are much larger than the $|A_\tau| \approx 50 \text{ GeV}/c^2$ at the electroweak scale given by the assumption of a common trilinear coupling at the GUT scale, $A_0 = 0$. Values of $|A_\tau| \approx 50 \text{ GeV}/c^2$ do not influence the limit at all, as they are much smaller than the $\mu \tan\beta$ values in the region of the limit.

However, in a pathological model where there is no mass in the sbottom or stop sector ($A_b = \mu \tan\beta$, $A_t = \mu/\tan\beta$) but only in the stau sector, one can make $\tilde{\tau}_1$ degenerate with $M_{\tilde{\chi}_1^0}$ even for high values of m_0 and $|\mu|$ so that the $\tilde{\chi}_1^0 \tilde{\chi}_2^0$ production cross-section at LEP is very small, and the production of the Higgs boson and other sfermions is not accessible kinematically.

3.3. $\tilde{\chi}_1^\pm$, $\tilde{\chi}_2^0$, $\tilde{\chi}_3^0$, and $\tilde{\chi}_4^0$ mass limits for any m_0

Fig. 7 shows the chargino mass limit as a function of $\tan\beta$ for $M_2 < 200 \text{ GeV}/c^2$. The lowest non-excluded chargino mass is found at MSSM points very close to those giving the LSP mass limit, and the arguments presented in Section 3.2.1 also to explain the dependence of the chargino mass limit on $\tan\beta$. For $\tan\beta \leq 1.2$ the limit occurs at high m_0 values. For $1.4 \lesssim \tan\beta \lesssim 4$ and $M_2 < 200 \text{ GeV}/c^2$, the limit occurs at low m_0 in the chargino-sneutrino degeneracy region. It rises slightly at $\tan\beta \gtrsim 4$, and

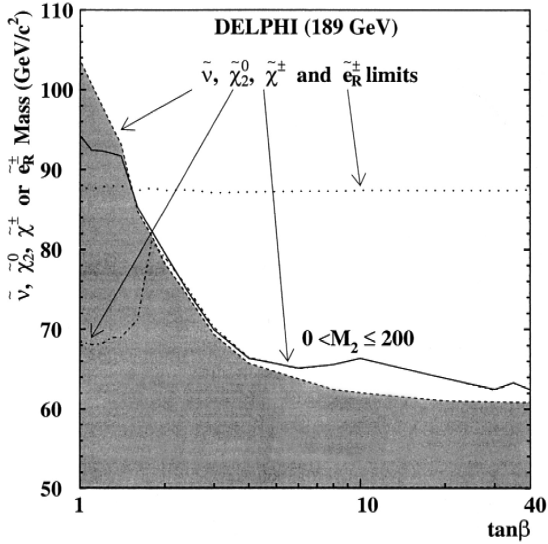


Fig. 7. The minimum sneutrino mass (dark shading and the dashed curve) allowed by the slepton and neutralino searches, as a function of $\tan\beta$, together with the limits on the chargino mass (solid curve), next-to-lightest neutralino mass (dash-dotted curve) and the \tilde{e}_R mass (dotted curve and the light shading). For $\tan\beta \geq 1.8$ the next-to-lightest neutralino mass limit (dash-dotted curve) and the chargino mass limit (dotted curve) occur in the LSP limit points for high $|\mu|$, where $M_{\tilde{\chi}_2^0} \approx M_{\tilde{\chi}_1^\pm}$. Therefore the dash-dotted curve follows the solid curve for $\tan\beta \geq 1.8$. The sneutrino and selectron mass limits were obtained assuming no mass splitting in the third sfermion family ($A_\tau - \mu \tan\beta = 0$ in particular). The selectron mass limit is valid for $M_{\tilde{e}_R} - M_{\tilde{\chi}_1^0} > 10 \text{ GeV}/c^2$.

then falls back for $\tan\beta \geq 10$ because of the small $\Delta M = M_{\tilde{\tau}} - M_{\tilde{\chi}_1^0}$.

The lightest chargino is constrained to have a mass:

$$M_{\tilde{\chi}_1^\pm} > 62.4 \text{ GeV}/c^2.$$

This limit is valid for any m_0 , $M_2 < 200 \text{ GeV}/c^2$ and $1 \leq \tan\beta \leq 40$, and it occurs in the region of the neutralino-stau degeneracy for $\tan\beta = 40$. It coincides with the one obtained at very high M_2 (see subsection 3.1) in the chargino-neutralino degeneracy region. Thus the chargino is bound to be heavier than $M_{\tilde{\chi}_1^\pm} > 62.4 \text{ GeV}/c^2$ for any m_0 and M_2 values and $1 \leq \tan\beta \leq 40$.

The mass of the next-to-lightest neutralino has to satisfy (see Fig. 7):

$$M_{\tilde{\chi}_2^0} > 62.4 \text{ GeV}/c^2.$$

The limit occurs at the same MSSM point as the chargino mass limit and it is valid for any m_0 and M_2 values and $1 \leq \tan\beta \leq 40$.

The masses of the $M_{\tilde{\chi}_3^0}$ and $M_{\tilde{\chi}_4^0}$ have to satisfy: $M_{\tilde{\chi}_3^0} > 99.9 \text{ GeV}/c^2$ and $M_{\tilde{\chi}_4^0} > 116.0 \text{ GeV}/c^2$.

These limits occur at $\tan\beta = 1$, close to the MSSM point of the LSP limit for high m_0 , and they are valid for any m_0 and M_2 values and $1 \leq \tan\beta \leq 40$.

3.4. $\tilde{\nu}$ and \tilde{e}_R mass limits for any m_0

The sneutrino and the \tilde{e}_R have to be heavier than: $M_{\tilde{\nu}} > 61 \text{ GeV}/c^2$ and $M_{\tilde{e}_R} > 87 \text{ GeV}/c^2$.

These shown in Fig. 7, were obtained assuming no mass splitting in the third sfermion family ($A_\tau = \mu \tan\beta$), implying $M_{\tilde{e}_R} = M_{\tilde{\tau}_R} = M_{\tilde{\tau}_1} = M_{\tilde{\mu}_R}$, as this gives the lowest values. If mass splitting in the stau sector is present (in the form $A_\tau - \mu \tan\beta$) and $A_\tau = 0$, the sneutrino mass limit rises to $M_{\tilde{\nu}} > 64 \text{ GeV}/c^2$, as $\tilde{\tau}_1$ pair-production puts a constraint on the sneutrino mass. Moreover, low m_0 (and thus low $M_{\tilde{e}_R}$ and $M_{\tilde{\nu}}$) values are not allowed at high $\tan\beta$ if the lightest neutralino is the LSP (see Fig. 6).

These limits result from the combination of slepton and neutralino searches. The selectron mass limit (see Fig. 7, dotted curve) is valid for $-1000 \text{ GeV}/c^2 \leq \mu \leq 1000 \text{ GeV}/c^2$ and $1 \leq \tan\beta \leq 40$ provided that $M_{\tilde{e}_R} - M_{\tilde{\chi}_1^0} > 10 \text{ GeV}/c^2$, and it allows a limit to be set on the sneutrino mass as shown in Fig. 7 (dashed curve). The sneutrino mass limit is expected to rise for $\tan\beta < 1$, the sneutrino being heavier than the \tilde{e}_R for small $\tan\beta$. If $M_{\tilde{e}_R} - M_{\tilde{\chi}_1^0} < 10 \text{ GeV}/c^2$, the most unfavourable situation appears when $\tilde{\chi}_1^+ \tilde{\chi}_1^-$ and $\tilde{\chi}_2^0 \tilde{\chi}_1^0$ production are kinematically inaccessible and the splitting between $M_{\tilde{e}_R}$ and $M_{\tilde{e}_L}$ is sufficiently large to make $\tilde{e}_R \tilde{e}_L$ production inaccessible as well. In this case the lower limit on $M_{\tilde{e}_R}$ is about $70 \text{ GeV}/c^2$ but the limit on the sneutrino mass does not deteriorate, as $M_{\tilde{\nu}}$ is high. For $\tan\beta \leq 1.4$ the sneutrino and the \tilde{e}_R mass limits occur at points where neither chargino nor neutralino production is kinematically accessible. For larger $\tan\beta$ they occur at the points of the LSP limit (Fig. 6). The selectron mass limit for $\tan\beta = 1.5$ and $\mu = -200 \text{ GeV}/c^2$ was presented in [2].

4. Summary and perspective

Searches for sleptons, charginos and neutralinos at centre-of-mass energies up to $\sqrt{s} = 188.7 \text{ GeV}$ set

lower limits on the masses of the supersymmetric particles.

Within the Minimal Supersymmetric Standard Model with gauge mass unification and sfermion mass unification at the GUT scale, the lightest neutralino has been constrained to have a mass $M_{\tilde{\chi}_1^0} > 32.3 \text{ GeV}/c^2$.

The lightest chargino $\tilde{\chi}_1^\pm$, the second-to-lightest neutralino $\tilde{\chi}_2^0$, the $\tilde{\chi}_3^0$, the $\tilde{\chi}_4^0$, the sneutrino $\tilde{\nu}$, and the \tilde{e}_R were found to be heavier than $62.4 \text{ GeV}/c^2$, $62.4 \text{ GeV}/c^2$, $99.9 \text{ GeV}/c^2$, $116.0 \text{ GeV}/c^2$, $61.0 \text{ GeV}/c^2$, and $87 \text{ GeV}/c^2$ respectively. These limits do not depend on m_0 or M_2 , and are valid for $1 \leq \tan\beta \leq 40$, in the μ range where the lightest neutralino is the LSP. If the sneutrino is heavier than the chargino, the lightest neutralino has to be heavier than $32.4 \text{ GeV}/c^2$. The effects of mixing in the third family of sfermions on these limits have been discussed. The search for $\tilde{\chi}_1^0 \tilde{\chi}_2^0$ and $\tilde{\chi}_2^0 \tilde{\chi}_2^0$ production with $\tilde{\chi}_2^0 \rightarrow \tilde{\tau} \tau$ was exploited in setting the limits. No significant dependence of the above mass limits on the mixing in the stau sector was found.

The branching fractions of the decays of heavier neutralinos depend on the mass of the lightest Higgs boson (h^0), which in turn depends on the mixing in the stop sector (A_t), and the mass of the pseudoscalar boson A^0 within the model used. Nevertheless, the dependence of the efficiency of the neutralino searches on h^0 production is weak, and no dependence of the limits on the mass of the lightest Higgs boson was found.

Other LEP experiments, using their data sets collected concurrently with the ones used in this work, have reported similar limits on the masses of the lightest neutralino and the lightest chargino [19–21]; the ALEPH [19] and OPAL [21] results were obtained assuming no mixing in the stau sector.

If there is no discovery of supersymmetry at LEP, one can expect the $0.5 < \tan\beta < 2$ range to be excluded by Higgs searches [22] and, for high m_0 , the lightest chargino will be excluded up to the kinematical limit. The LSP limit for high m_0 would then occur at $\tan\beta = 2$, and the limit on the chargino mass $M_{\tilde{\chi}_1^\pm} > 102 \text{ GeV}/c^2$ would result in $M_{\tilde{\chi}_1^0} > 49 \text{ GeV}/c^2$. For low m_0 and $\tan\beta \lesssim 8$, the LSP limit depends primarily on the mass limit on the right-handed selectron: $M_{\tilde{e}_R} > 97 \text{ GeV}/c^2$ would result in $M_{\tilde{\chi}_1^0} > 47 \text{ GeV}/c^2$ for $2 < \tan\beta \lesssim 8$. In

[23], presently available preliminary results from LEP and the Tevatron, together with constraints from $b \rightarrow s \gamma$ decay, were already used to set similar limits on $\tan\beta$ ($\tan\beta > 1.9$) and $M_{\tilde{\chi}_1^0}$ ($M_{\tilde{\chi}_1^0} > 46 \text{ GeV}/c^2$).

Acknowledgements

We are greatly indebted to our technical collaborators, to the members of the CERN-SL Division for the excellent performance of the LEP collider, and to the funding agencies for their support in building and operating the DELPHI detector. We acknowledge in particular the support of the Austrian Federal Ministry of Science and Traffics, GZ 616.364/2-III/2a/98, FNRS-FWO, Belgium, FINEP, CNPq, CAPES, FUJB and FAPERJ, Brazil, Czech Ministry of Industry and Trade, GA CR 202/96/0450 and GA AVCR A1010521, Danish Natural Research Council, Commission of the European Communities (DG XII), Direction des Sciences de la Matière, CEA, France, Bundesministerium für Bildung, Wissenschaft, Forschung und Technologie, Germany, General Secretariat for Research and Technology, Greece, National Science Foundation (NWO) and Foundation for Research on Matter (FOM), The Netherlands, Norwegian Research Council, State Committee for Scientific Research, Poland, 2P03B06015, 2P03B03311 and SPUB/P03/178/98, JNICT-Junta Nacional de Investigação Científica e Tecnológica, Portugal, Vedecka grantova agentura MS SR, Slovakia, Nr. 95/5195/134, Ministry of Science and Technology of the Republic of Slovenia, CICYT, Spain, AEN96-1661 and AEN96-1681, The Swedish Natural Science Research Council, Particle Physics and Astronomy Research Council, UK, Department of Energy, USA, DE-FG02-94ER40817.

References

- [1] P. Fayet, S. Ferrara, Phys. Rep. 32 (1977) 249; H.P. Nilles, Phys. Rep. 110 (1984) 1; H.E. Haber, G.L. Kane, Phys. Rep. 117 (1985) 75.
- [2] DELPHI Collaboration, Searches for Sleptons at $\sqrt{s} = 183$ to 189 GeV , to be submitted to Eur. Phys. J.C.

- [3] DELPHI Collaboration, P. Abreu et al., Phys. Lett. B 387 (1996) 651.
- [4] DELPHI Collaboration, P. Abreu et al., Eur. Phys. J. C (1), 1998, p. 1.
- [5] DELPHI Collaboration, P. Abreu et al., Phys. Lett. B 446 (1999) 75.
- [6] DELPHI Collaboration, Search for neutralinos at 189 GeV, to be submitted to Phys. Lett. B.
- [7] DELPHI Collaboration, P. Abreu et al., Eur. Phys. J. C 6 (1999) 371.
- [8] DELPHI Collaboration, P. Abreu et al., Phys. Lett. B 382 (1996) 323.
- [9] DELPHI Collaboration, Phys. Lett. B 479 (2000) 118.
- [10] DELPHI Collaboration, Update of the search for charginos nearly mass-degenerate with the lightest neutralino, CERN-EP-2000-033, submitted to Phys. Lett. B.
- [11] DELPHI Collaboration, P. Abreu et al., Phys. Lett. B 380 (1996) 471.
- [12] A. Bartl, H. Fraas, W. Majerotto, Z. Phys. C 30 (1986) 441; A. Bartl, H. Fraas, W. Majerotto, Z. Phys. C 41 (1988) 475; A. Bartl, H. Fraas, W. Majerotto, B. Mösslacher, Z. Phys. C 55 (1992) 257.
- [13] S. Ambrosanio, B. Mele, Phys. Rev. D 52 (1995) 3900; S. Ambrosanio, B. Mele, Phys. Rev. D 53 (1996) 2451.
- [14] DELPHI Collaboration, Searches for Neutral Higgs Bosons in e^+e^- Collisions around $\sqrt{s} \leq 189$ GeV, CERN-EP-2000-038, Accepted by E. Phys. J.C.
- [15] DELPHI Collaboration, A search for invisible Higgs bosons produced in e^+e^- interactions up to $\sqrt{s} = 189$ GeV, CERN-EP-2000-051, submitted to Phys. Lett. B.
- [16] S. Katsanevas, S. Melachroinos in Physics at LEP2, CERN 96-01, vol. 2, p. 328; S. Katsanevas, P. Morawitz, Comp. Phys. Comm. 122 (1998) 227.
- [17] V.F. Obraztsov, Nucl. Instr. and Meth. 316 (1992) 388; Nucl. Instr. and Meth. 399 (1997) 500 (E).
- [18] LEPSUSYWG, ALEPH, DELPHI, L3 and OPAL experiments, note LEPSUSYWG/99-03.1.
- [19] ALEPH Collaboration, Search for Charginos and Neutralinos in e^+e^- Collisions at $\sqrt{s} = 188.6$ GeV and Mass Limit for the Lightest Neutralino, ALEPH 99-011 CONF 99-00.
- [20] L3 Collaboration, M. Acciarri et al., Phys. Lett. B 472 (2000) 420.
- [21] OPAL Collaboration, G. Abbiendi et al., Search for Chargino and Neutralino Production at $\sqrt{s} = 189$ GeV at LEP, CERN-EP/99-123, Accepted by Eur. Phys. J.C.
- [22] LEP Higgs Working Group, ALEPH, DELPHI, L3 and OPAL Collaborations, CERN-EP-2000-055.
- [23] J. Ellis, T. Falk, G. Ganis, K.A. Olive, Supersymmetric Dark Matter in the Light of LEP and the Tevatron Collider, CERN-TH/2000-106.